

# Flight Control with Distributed Effectors

Stefan R. Bieniawski\* and Ilan M. Kroo†  
*Stanford University, Stanford, CA 94305*

David H. Wolpert‡  
*NASA Ames Research Center, Moffett Field, CA 94035*

Recent developments in actuator technology have resulted in small, simple devices capable of affecting the flow field over flight vehicles sufficiently to generate control forces. One of the devices which has been under investigation is the Miniature-Trailing Edge Effector (MiTE), which consists of a small, 1-5% chord, moveable surface mounted at the wing trailing edge. The high bandwidth and good control authority make the device an ideal candidate for control of both the rigid body and flexible modes of a flight vehicle. Unfortunately traditional control techniques do not address the non-linear nature of the device or the competing performance goals arising from large numbers of distributed devices. Novel approaches to control design are therefore required. To demonstrate the potential of this type of flight control architecture and to explore suitable control synthesis techniques, a remotely piloted flight vehicle has been developed. This paper details the flight vehicle including a distributed flight control system based upon MiTEs. The latter system includes distributed sensing, logic, and actuation. This paper also describes an applicable novel control synthesis technique based upon the theory of collectives. The theory and its application to the design of distributed flight control systems is presented. Results of flight tests with conventional control surfaces and with a MiTE based control system are provided.

## Introduction

VARIOUS actuation devices have been recently developed which can be used to locally affect the flow-field over flight vehicles sufficiently to generate control forces. Often constructed using meso- or smaller scale manufacturing processes and utilizing a variety of actuation technologies, these devices are small in size, low in cost, and typically binary in nature. These new devices offer many potential advantages for flight vehicle control, including robustness due to the large number of devices and simplicity through elimination of complicated servo-positioning. Furthermore, the high bandwidth and distributed placement of the new devices allows for structural as well as rigid body mode control.

Several researchers have been developing small devices for flow control.<sup>1,2</sup> At Stanford University re-

search in small flow control devices started in 1998 and has focused on Miniature-Trailing Edge Effectors (MiTEs).<sup>3-5</sup> The MiTEs are small trailing edge devices, approximately 1-5% chord in height, actuated with deflection angles up to 90 degrees. The MiTE concept is inspired by Gurney flaps originally developed and applied to racing cars by Robert Liebeck and Dan Gurney. These devices protrude vertically into the flow and cause a stable separation region to form changing the sectional lift and moment comparable to a traditional flap of much larger size.<sup>6</sup> Numerous wind tunnel tests<sup>3,5,7,8</sup> and CFD simulations<sup>3,9,10</sup> have confirmed the influence and behavior of small flaps. The motion of the MiTEs relative to the free-stream requires significantly smaller actuator force for a given change in sectional lift compared with a conventional flap. The lower aerodynamic moments, combined with the small device mass, results in high bandwidths, with designs achieving levels up to 40 Hz.

Although extensive aerodynamic testing has been completed with these types of small devices, re-

---

\*Doctoral Candidate, AIAA Member.

†Professor, AIAA Fellow.

‡Senior Research Scientist.

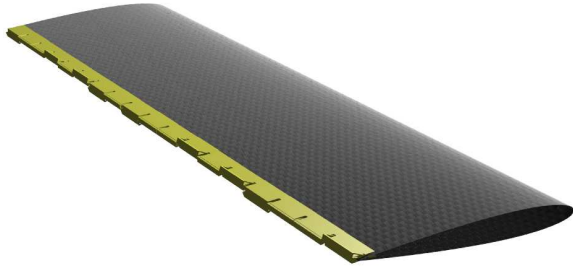


**Fig. 1 Concept wing with MiTE effectors.**

searchers are only beginning to address their potential for active control. One area of application that has been explored is the aeroelastic control of high aspect ratio wings. Recent experiments have demonstrated the capability of MiTEs as aeroelastic control devices, specifically to stabilize a wing operating beyond its flutter speed.<sup>11</sup> These experiments, however, have only addressed control with a limited number of devices and were performed with significant support equipment.

Other control challenges can be addressed with a distributed flight control system based upon the MiTEs. Figure 1 shows one concept in which the complete trailing edge is equipped with MiTEs. For example, the large number of devices allows for tailoring of the lift distribution at off-design flight conditions. This type of application is already being pursued by Airbus using an A340 equipped with miniature trailing edge devices.<sup>22</sup> The small, high-bandwidth devices can also alleviate gust loads, resulting in reduced structural weight. The devices also allow for arbitrary combinations of control forces and are ideal for configurations such as flying wings. Flying wings offer two further challenges which may be addressed by a MiTE based control. First, such configurations often experience coupling between the rigid body short period mode and the wing bending modes, resulting in degraded handling qualities or flutter. Second, the performance of flying wings is usually increased by flying with relaxed longitudinal static stability. A MiTE based distributed control architecture, with its high bandwidth and large number of devices, would be able to address these control challenges. As a step toward addressing these challenges, the current effort is focused on developing a suitable flight vehicle and demonstrating a flight ready MiTE based control system.

Researchers are also investigating MiTEs and related devices for application to rotorcraft<sup>12</sup> and wind turbines.<sup>13</sup> The developments presented in this work of a practical, flight ready, distributed control system based upon MiTEs can also be applied to these areas.

Traditional control techniques, however, do not address the nonlinear nature of the MiTEs or the com-

peting performance goals arising from potentially large numbers of distributed devices. The approach pursued in the current work is to distribute the control among agents located throughout the flight vehicle. Each agent consists of a number of effectors, control logic, and local sensors. The controller design becomes a distributed optimization for parameters governing the control policies that the individual agents will follow. Formulating the controller design in this manner allows for the application of techniques from machine learning, statistics, multi-agent systems, and game theory. The current work leverages these fields by applying Collective Intelligence (COIN) to the distributed control design. COIN is a framework for designing a “collective”, defined as a system of adaptive computational agents with a system-level performance criteria. COIN techniques have been applied to a variety of distributed optimization problems including network routing, computing resource allocation, and data collection by autonomous rovers.<sup>14–16</sup> Probability Collectives (PC) theory formalizes and substantially extends the COIN framework.<sup>17</sup> PC theory has been compared with results obtained with traditional COIN approaches<sup>19</sup> and has also been demonstrated on new problem domains.<sup>20,21</sup> This work applies PC theory to the design of distributed, nonlinear controllers robust to noise and disturbances.

The paper begins with a description of the flight demonstrator including the distributed flight control architecture based upon the MiTEs. The analytical model used for the control design is described along with comparisons of open-loop flight tests. The distributed controller design approach based upon Probability Collectives is then presented. The paper concludes with controller designs and flight test results.

## Flight Demonstrator

### General Description

To demonstrate the potential of novel distributed flight control architectures and to explore suitable control synthesis techniques, a remotely piloted flight vehicle has been developed. Figure 2 shows the flight demonstrator equipped with conventional control surfaces. The vehicle can be configured with either four conventional servo-actuated control surfaces or utilize a MiTE based distributed flight control system. The vehicle is a six foot span flying wing with 30 degree sweep on the outboard panels. The outboard sections are of constant chord set to 12 inches to accommodate MiTEs with 2% chord deflected height. The wing skins are manufactured from balsa core sandwich panels faced with carbon fiber and fiberglass. The vehicle has an electric powerplant composed of an advanced external rotor brushless motor driving a



**Fig. 2** View of flight vehicle.

10-by-6 inch folding propeller drawing current from a three cell Lithium Polymer battery pack. The vehicle is designed to fly efficiently at an overall lift coefficient of 0.7 through a combination of airfoil selection and wing washout. The flying weight of the conventional control configuration is 4.4 pounds.

Communication with the vehicle is accomplished using two separate radio frequency links, one for pilot commands, and the other for data. The vehicle is flown by a pilot using standard 72 MHz radio-control technology. The transmitted pilot commands are received and processed by a central micro-controller. In the case of the conventional configuration the commands are passed on unchanged to the servo-actuators. For both configurations, the commands are sent to a dedicated data logging system. The latter includes another micro-controller which combines the commanded pilot inputs with sampled measurements of airspeed, altitude, 3 axis angular rates, and 3 axis accelerations. The data is broadcast at 50 Hz to a ground station using a 900 MHz AeroComm serial radio. The ground station, comprised of a receiving AeroComm radio connected to a laptop, records the data.

The vehicle was tested in two configurations, free-flight and captive car testing. The only difference between the two configurations is the latter prevented the vehicle from displacing while allowing it to rotate about any axis. In all other respects, such as power, communication, and data acquisition, the configurations were identical. For the car-top testing the vehicle was mounted at its center of gravity to a frame which was then attached to a car, as shown in Figure 3. This provided a much more controlled environment for eval-



**Fig. 3** View of captive car testing configuration.

uating controller designs. The effects on the vehicle dynamics are discussed in more detail in section describing the analytical model.

### Distributed Control Architecture

The distributed control architecture is shown schematically in Figure 4. In this configuration the pilot commands received by the central micro-controller are broadcast to both the logging micro-controller and to the distributed agents through a communication and power bus running the length of the trailing edge. The power to the distributed agents is provided by centralized batteries, although the power supply could also be distributed through the airframe. The bus provides eight possible positions for the distributed agents including three positions in each outboard wing and two in the centerbody. A unique feature of the architecture is its modularity which allows all the agents to be interchanged and supports “hot-plugging” between the different positions. Although the flight vehicle is relatively small, the architecture and hardware developed for this experiment can easily be scaled to a much larger vehicle with little modification.

A close-up view of one of the distributed agents is shown in Figure 5 mounted in one of the centerbody positions. Each agent is comprised of two MiTE effectors, supporting logic and power conditioning circuitry, and an interface with a local sensor. Smaller MiTE devices and additional sensors could easily be incorporated without significant changes to the architecture. The complete agent measures 8.5 inches in length and 1.75 inches in depth. The MiTE devices have been manufactured to conform into the

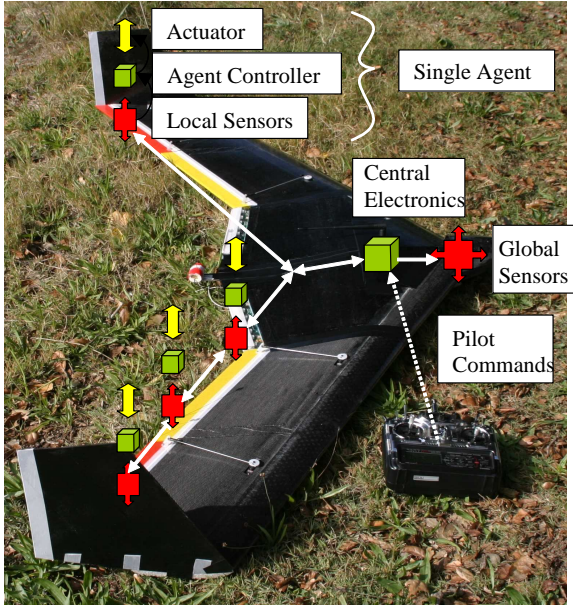


Fig. 4 Distributed flight control architecture.



Fig. 5 MiTE based “agent” in flight configuration.

trailing edge shape, leaving a clean aerodynamic surface when not actuated. The agent logic consists of a micro-controller which processes the broadcast pilot commands, fuses this with the locally sensed data, and commands the positions of the MiTEs. For the closed-loop experiments described later, the local sensors consisted of single axis accelerometers although other sensors could be used for different applications.

The MiTEs are actuated using small DC pager motors and are capable of either two or three states, depending upon the configuration. Due to the small size, high bandwidth, and simple mechanism, no positioning feedback is required. For increased bandwidth the MiTEs are paired such that one deflects neutral-down while the other neutral-up. This configuration was used in the successful flutter suppression tests.<sup>11</sup> Alternatively each MiTE can achieve three states: up, down, and neutral through either kinematic design or with a centering spring. A variant capable of three states was used for the tests during this work.

## Analytical Model

### Flight Configuration

A linear aerodynamic model was generated in LinAir<sup>23</sup> and stability derivatives were obtained. For the conventional configuration, the control surfaces were modelled as plain flaps. Two surfaces were located on each wing and were deflected in unison. Mixing of the pilot commands was performed within the remote-controlled transmitter. The result was to have the surfaces perform both the elevator and aileron functions. For modelling purposes the conventional inputs were then elevator and aileron, allowing the equations of motion to be decoupled.

The MiTEs are also modelled as plain flaps by matching the steady sectional lift and pitching moment increments. Steady thin airfoil theory provided the equivalent flap chord percentage and angle of deflection to model the MiTEs. The flight vehicle geometry result in devices with 2% chord deflected height. Based upon previous computational and experimental results<sup>7,10</sup> the expected force and moment increments are:  $\Delta C_l = 0.4$  and  $\Delta C_{mac} = -0.10$ . These are approximated using thin airfoil theory with flap chord percentage  $c_f/c = 0.125$  and  $\delta_{max} = 8.9$  degrees. The conventional control configuration has the same flap chord percentage but is capable of much higher deflection angles. The linear model provided the aerodynamic control forces on the vehicle generated by the MiTE equivalent deflection. These results, along with the computed stability derivatives and mass properties obtained from tests, are combined into the equations of motion.<sup>24</sup> The resulting system equations are of the form,

$$\begin{aligned} x^{(k+1)} &= [A]x^{(k)} + [B]u^{(k)} + w \\ y^{(k)} &= [C]x^{(k)} + v \\ u^{(k)} &= [u_1^{(k)} \quad u_2^{(k)} \quad \dots \quad u_N^{(k)}]^T \end{aligned} \quad (1)$$

where  $v$  and  $w$  are the noise and disturbance, respectively. The non-linearity in the system results from discrete commanded positions,  $u_i$ , of the MiTEs.

### Car Test Configuration

A significant portion of the quantitative testing was performed with the flight vehicle mounted to an automobile, as shown previously in Figure 3. A ball joint was located at the center of gravity and allowed the vehicle to rotate about all three axes without displacing. The actual point of rotation was located slightly below the center of gravity. The aerodynamic effects of the automobile on the flight vehicle dynamics were neglected. The effect of constraining the displacements and the vertical offset on the dynamics were however considered.

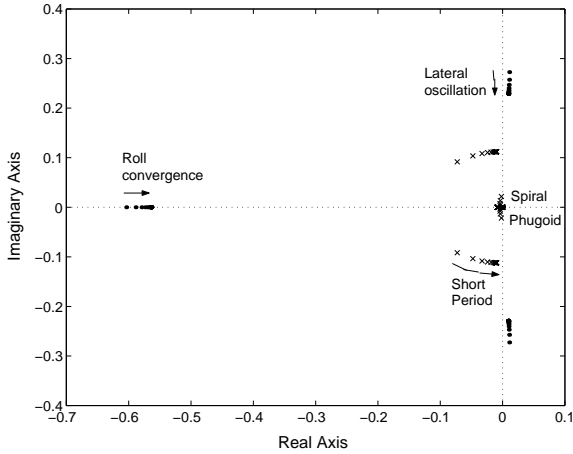


**Fig. 6 Root locus versus increasing mass.**

Following<sup>25</sup> one way to model the effect of constraining the flight vehicle is to increase the mass ratio. In the limit this will result in the same set of equations derived with the center of gravity constrained. It is, however, informative to examine the root locus as the mass ratio is increased to observe the changes in the system dynamics.

The root locus versus increasing the mass ratio is shown in Figure 6. The phugoid pole moves quickly towards the origin rapidly decreasing its frequency. In the limit this pole can be eliminated from the system of equations. Since this mode is typically corrected for by the pilot its absence will have little effect upon the test results. The short period mode is seen to significantly decrease in damping while only slightly changing in natural frequency. In the limit, however, the mode is still stable. The other important pole is the lateral oscillation which decreases in frequency with increasing mass ratio. The mode remains slightly unstable. These differences in the dynamics indicate that any testing performed in the captive configuration will be conservative when compared with actual flight.

The lateral mode is further destabilized by the effect of the vertical offset between the c.g. and the center of rotation of the ball joint. To counter this effect during the cartop tests, the wingtips were modified either by inverting the baseline winglets or through an added anhedral element. These slightly lowered the c.g. and increased the damping of the lateral oscillation by aerodynamic means.

## Open Loop Tests

### Captive Car-top Tests

Captive cartop tests were performed with the flight vehicle equipped with both conventional control surfaces and with the MiTEs. The modified wingtip configurations were used during the tests to stabilize

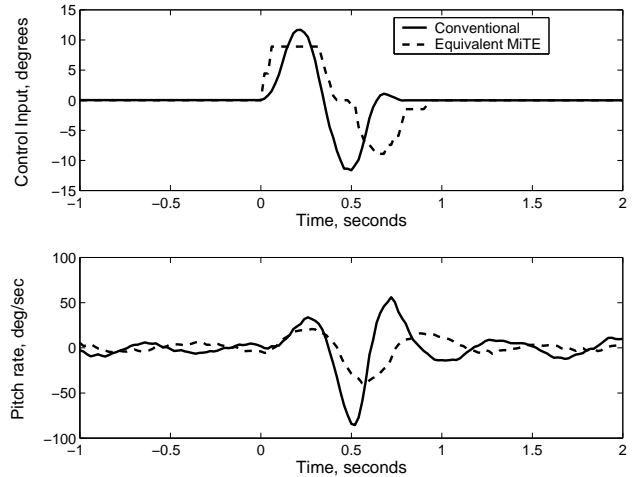


**Fig. 7 Comparison of longitudinal responses.**

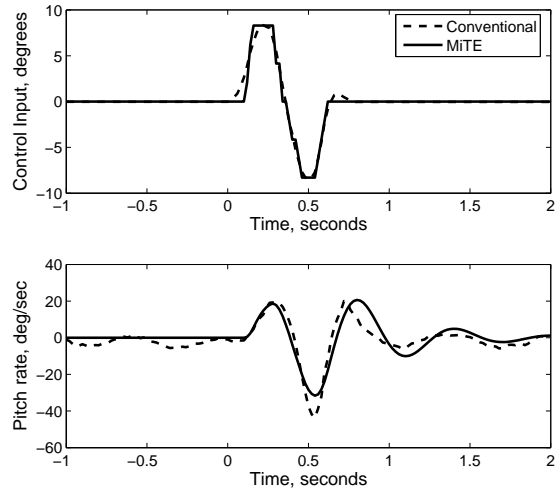


**Fig. 8 Corrected comparison of longitudinal responses.**

the vehicle dynamics and provide a better indication of the effect of the control input. Inertial properties were also significantly different due to the higher mass of the MiTE actuators and the requirements for maintaining the overall vehicle center of gravity position. The pitch inertia, for example, increased 14%, while the roll inertia increased 8%.

The response to elevator doublets are compared in Figure 7. The data shown for each configuration is the averaged response over multiple doublets. The MiTE input is scaled to the equivalent conventional input. Differences in the vehicle dynamics, control input amplitude, and control input time history result in a larger response for the conventional configuration. To provide a more direct comparison and to validate the effect of the MiTEs on the vehicle dynamics, system identification was performed on the data obtained

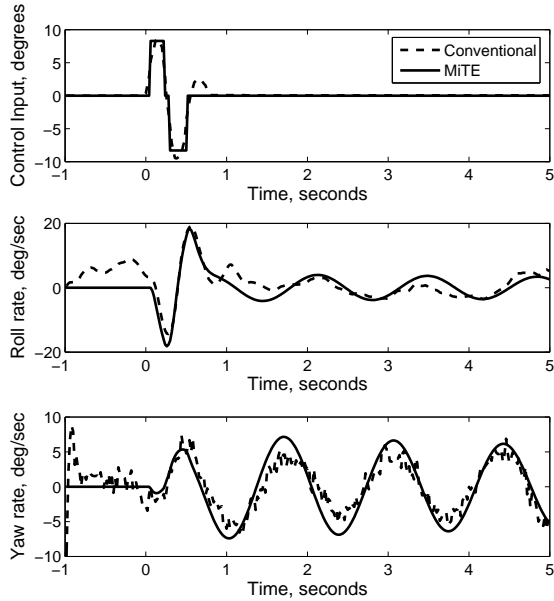


**Fig. 9** Corrected comparison of lateral responses.

for both configurations. The identified models were then used to remove the differences in the dynamics. Differences in the input time histories were removed by converting the conventional input into an equivalent MiTE input and simulating the response using the identified dynamics. This comparison is shown in Figure 8. A similar scaled and corrected comparison of the lateral response is shown in Figure 9. Both show good agreement, validating both the influence of the MiTEs on the vehicle dynamics and the analytical model. The resulting models are now also suitable for the design of controllers to utilize the MiTEs.

### Distributed Controller Design

In general at each time step  $k$  a controller uses the current and  $N$  previous measurements  $\{y(k), y(k-1), \dots, y(k-N)\}$ , to determine the control inputs,  $u_i(k)$ , for each actuator  $i$ . This mapping is the control policy,  $\pi_i$ , for actuator  $i$ , and is defined as,

$$\pi_i : f(\vec{Y}_i) \rightarrow u_i \quad (2)$$

where  $\vec{Y}_i$  is referred to as the feature vector with  $Y_i$  being combinations of the measurements available to  $i$ ,  $y_i$ . Note that these combinations can be nonlinear. In linear control for example, the control policies are linear combinations of the most recent measured outputs mapped into continuous control inputs. In general the control policies may use nonlinear combinations of current and previous measurements and map to discrete control inputs. The latter characteristic in particular is important for control design with the Miniature Trailing Edge (MiTE) effectors.

The control synthesis goal is to search for policies which minimize a specified objective function of the system states  $x(k)$ , and control inputs  $u(k)$ , subject to the system dynamics over some time horizon  $k = 1..T$ . In discrete time linear quadratic regulation (LQR), for example, this function is given by,

$$J(\pi) = \sum_{k=1}^T x(k)^T [Q] x(k) + u(k)^T [R] u(k)$$

where the matrices  $[Q]$  and  $[R]$  are used to weight the importance of the responses versus the control effort. The system dynamics act as constraints and are given by,

$$\begin{aligned} x(k+1) &= [A] x(k) + [B] u(k) \\ y(k) &= [C] x(k) + [D] u(k) \end{aligned}$$

with the control input  $u(k)$  given by the linear relation,

$$u(k) = [K] x(k)$$

In general, however, the objective function can be arbitrary. For example consider stabilizing the dynamics of an aircraft with multiple control surfaces while minimizing the profile and induced drag associated with that effort. The drag is a nonlinear function of the combination and amount the surfaces are deflected. In the aeroelastic control experiments,<sup>11</sup> the goal was to stabilize a flexible wing beyond its critical aeroelastic flow speed. In this case a suitable objective is to maximize the controllable flow speed. These objective functions are no longer quadratic and thus can not be addressed by LQR, even if the system were linear.

The control design must also address two additional features. First is the presence of noise and disturbance. Linear quadratic gaussian (LQG) control extends LQR to account for noise and disturbance, although this requires a Kalman filter to provide estimates of the states from the observed measurements. A model for the system dynamics must also be assumed. Second is the distributed nature of systems. This causes each actuator to have a limited amount of information or some added dynamics are associated with the information gathering, for instance transmission delays.

For LQR and LQG, the optimal control policy is found by solving the algebraic Riccati equation, but for general objectives and for nonlinear policies, an optimization approach is required. The disadvantage is the associated computational cost of the optimization technique which may involve numerous simulations or the system. Further, there is a large amount of literature, techniques, and practical experience associated with linear control design. The challenges and

potential of designing nonlinear, robust, distributed controllers with arbitrary objective functions however warrants exploration of the optimization approach. Optimization also allows for simple policies to be considered that can then be implemented easily in hardware. Probability Collectives provides an approach for performing this optimization and is especially well suited to problems that are distributed, nonlinear, and for which robust solutions are sought.

### Overview of Probability Collectives Theory

Probability Collectives (PC) theory formalizes and substantially extends the Collective Intelligence (COIN) framework.<sup>17</sup> The COIN solution process begins by assigning agents to the variables in the optimization problem. The agents then select actions and receive rewards based upon the system objective.<sup>16</sup> These rewards are then used by the agents to determine their next choice of action. The process reaches an equilibrium when the agents can no longer improve their rewards by changing actions. This approach is similar to many other methods in reinforcement learning (RL).<sup>26</sup> The core insight of PC theory, in contrast to COIN and RL techniques, is to concentrate on how the agents update the probability distributions across their possible actions rather than specifically on the joint action generated by sampling those distributions.

One way to view PC theory is as an extension of conventional game theory. In any game, the agents are independent, with each agent  $i$  choosing its move  $x_i$  at any instant by sampling its probability distribution (mixed strategy) at that instant,  $q_i(x_i)$ . Accordingly, the distribution of the joint-moves is a product distribution,  $P(x) = \prod_i q_i(x_i)$ . In this representation, all coupling between the agents occurs indirectly; it is the separate distributions of the agents that are coupled, while the actual moves of the agents are independent. Bounded rational agents balance their choice of best move with the need to explore other possible moves. Information theory shows that the equilibrium of a game played by bounded rational agents is the optimizer of a Lagrangian of the probability distribution of the agents' joint-moves.<sup>17,18</sup> Since the joint probability distribution is still a product, the optimization of the Lagrangian can be done in a completely distributed manner.

### Optimization Approach

Consider the unconstrained optimization problem,

$$\min_{\vec{x}} J(\vec{x})$$

where each agent sets one component of  $\vec{x}$  as that agent's action and the  $x_i$  are discrete. The Lagrangian<sup>17</sup>  $\mathcal{L}_i(q_i)$  for each agent as a function of the

probability distribution across its actions is,

$$\begin{aligned} \mathcal{L}_i(q_i) &= E[J(x_i, x_{(i)})] - T S(q_i) \\ &= \int dx_i q_i(x_i) E[J(x_i, x_{(i)})|x_i] - T S(q_i) \end{aligned}$$

where  $J$  is the world utility (system objective) which depends upon the action of agent  $i$ ,  $x_i$ , and the actions of the other agents,  $x_{(i)}$ , and  $T$  is referred to as the temperature. The expectation  $E[J(x_i, x_{(i)})|x_i]$  is evaluated according to the product distribution of the agents other than  $i$ :

$$P(x_{(i)}) = \prod_{j \neq i} q_j(x_j)$$

The entropy  $S$  is given by:

$$S(q_i) = - \int dx_j q_i(x_j) \ln q_i(x_j)$$

Each agent then addresses the following local optimization problem,

$$\begin{aligned} \min_{q_i} \mathcal{L}_i(q_i) \\ \text{s.t.} \quad \int dx_i q_i(x_i) = 1, \quad q_i(x_i) \geq 0, \forall x_i \end{aligned}$$

where the constraints to ensure the  $q_i$  are valid probabilities.

The Lagrangian is composed of two terms weighted by the temperature  $T$ : the expected reward across  $i$ 's actions, and the entropy associated with the probability distribution across  $i$ 's actions. During the minimization of the Lagrangian, the temperature provides the means to trade-off exploitation of good actions (low temperature) with exploration of other possible actions (high temperature).

The minimization of the Lagrangian is amenable to solution using gradient descent or Newton updating since both the gradient and the Hessian are obtained in closed form.<sup>18</sup> Performing the Lagrangian minimization involves a separate conditional expected utility for each agent. These are estimated either exactly if a closed form expression is available or with Monte-Carlo sampling if no simple closed form exists. In Monte Carlo sampling the agents repeatedly and jointly IID (identically and independently distributed) sample their probability distributions to generate joint moves, and the associated objective values are recorded. The Probability Collectives approach includes techniques for improving the efficiency of the sampling process.<sup>18</sup> In the context of control design each sample is equivalent to a single simulation of the system with each agent selecting a policy by sampling

from its distributions and using that policy throughout the simulation. Noise and disturbances are similarly sampled from their distributions and can therefore be viewed as additional agents who are not updating their distributions.

The detailed mathematical foundations of the Probability Collectives approach are provided in Wolpert, et al.<sup>17,18</sup> The algorithm for implementing the approach on a variety of optimization problems is described in Bieniawski, et al.<sup>21</sup>

### Detailed Formulation

The controller synthesis using the Probability Collectives begins by defining how the agent policies map from the features available to agent  $i$ ,  $y_i$ , to the agent control input,  $u_i$ . In the current work the agent policies follow a threshold function with a vector of weights  $\theta_i$  assigned to the features,

$$u_i = \begin{cases} +1 & \theta_i^T y \geq 1 \\ 0 & \text{otherwise} \\ -1 & \theta_i^T y \leq -1 \end{cases}$$

The features can include global or local sensor values or the actions of other agents. In the current work the features consist only of local sensor measurements so no communication is considered between the agents. Note that the agent actions are assumed to be symmetric, that is, for a given set of features  $y$  which resulted in command  $u$ , the negative would result in the command  $-u$ .

The next step is to define the objective of the control synthesis. For the current work the objectives similar to linear quadratic control are specified,

$$J(\pi) = \sum_{k=1}^T y(k)^T [Q] y(k) + u(k)^T [R] u(k) \quad (3)$$

where the matrices  $[Q]$  and  $[R]$  weight the importance of the responses versus the control effort. The system dynamics are also assumed to be linear and are given by Eqn. 1. The remaining nonlinearity in the system is due to the discrete possible commanded actuator positions.

The controller design is now reduced to the following unconstrained optimization,

$$\min_{\theta_1 \dots \theta_N} V(\pi)$$

which can be performed in a distributed manner using the Probability Collectives approach. Distributions for the noise, disturbance, and initial conditions are sampled each time the system is simulated. Note that although discrete time dynamics are shown the approach is just as well suited for nonlinear dynamics

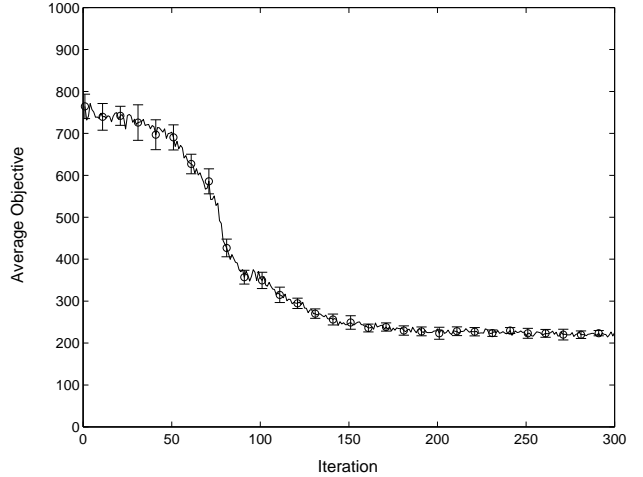


**Fig. 10** Convergence of objective for distributed controller.

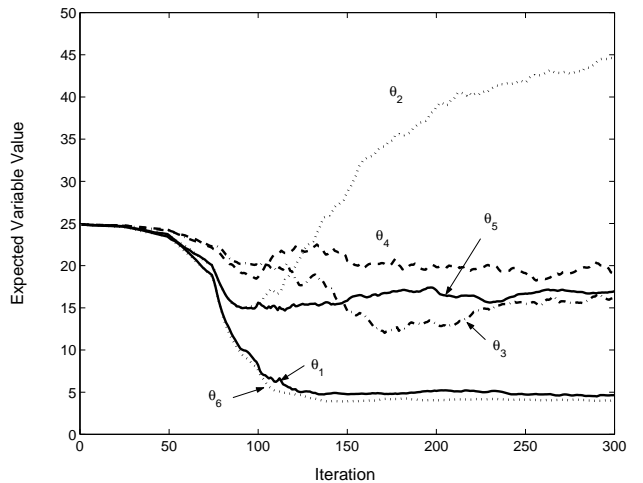


**Fig. 11** Convergence of one instance of variables.

since all that is required is a simulation and a resultant value for the objective.

## Results

To illustrate the distributed control design approach a distributed stability augmentation system was designed. Each of the agents located on the outboard sections of the flight vehicle are provided with local measurement of the vertical velocity. Each then utilizes a single parameter threshold policy to minimize the objective function given by Eqn. 3. Weights of  $Q=0.1$  and  $R=0.1$  were used. The resulting optimization has six total variables and was performed in a distributed manner using the Probability Collectives approach. For each simulation performed during the optimization, initial conditions were assigned as a vector of body rates of random direction and magnitude equal to 20 deg/sec.

The optimization was repeated 10 times to study

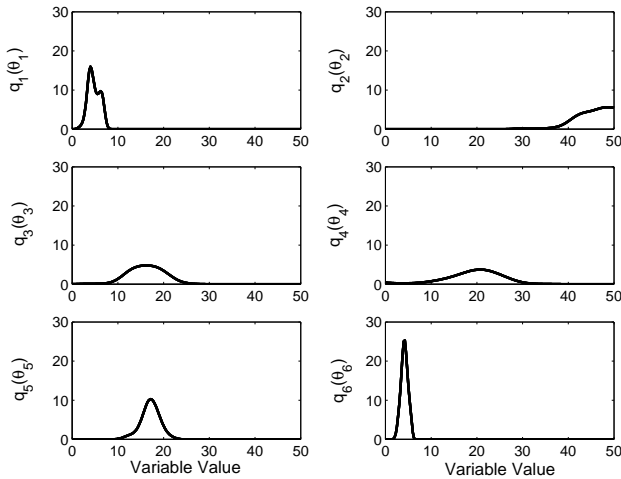


**Fig. 12** Probability distributions after 300 iterations.

the convergence behavior of the approach. Figure 10 shows the iteration history of the objective function. The mean and error bars indicating the standard deviation are shown. Each iteration used 10 simulations of the system. Other details and parameter settings for the optimization are available in Bieniawski.<sup>27</sup> Each optimization resulted in similar values for the objective function although quite differing values were obtained for the variables. This indicates there are many possible solutions, which can be expected. The variable iteration history is shown for a single case in Figure 11. Note that the resulting controller is not symmetric implying that the controller is coupling the lateral and longitudinal responses. The Probability Collectives approach explicitly uses probability distributions that can be studied to determine the sensitivity of the optimum. Figure 12 shows the distributions for the variables after 300 iterations. They indicate that variables 1 and 6, the outermost agents, are most important with the other agents being allowed quite a large variation.

Figure 13 shows a comparison of the open loop and closed loop time histories for the vehicle angular rates. The controller is seen to dramatically decrease the pitch and roll response and to also decrease the yaw response. Note that the objective function only considered the roll and pitch rates through weights on the vertical velocity so no effort was made to minimize the yaw rate.

### Closed Loop Tests

Closed loop tests were performed with the flight vehicle in the captive car top configuration. The distributed controllers used locally sensed accelerations and independent decision making. The controllers were intended to provide stability augmentation, par-

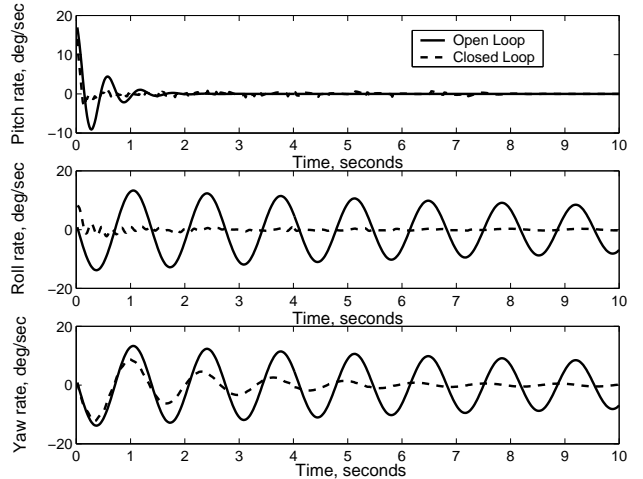


**Fig. 13** Comparison of open and closed loop response.

	Root mean square responses, deg/sec		
	Pitch rate	Roll rate	Yaw rate
Open loop	11.1	17.2	18.1
Closed loop	14.8	15.7	12.3
Difference	+33%	-9%	-33%

**Table 1** Results of initial tests with distributed stability augmentation system.

ticularly for the lateral oscillation mode of the flight vehicle.

In the experiments, the two outboard agents were provided with local vertical accelerations that were then integrated and filtered to provide vertical velocities. A single gain was applied to the local velocities and the resulting quantity combined with commanded pilot inputs. If the total exceeded a specified threshold both MiTEs belonging to the agent were actuated in unison. Table 1 provides an initial comparison of the performance with the distributed controllers on and with them off. Listed are the root-mean-square values for the flight vehicle angular rates. A significant decrease in the response of the lateral mode is obtained. The response of the longitudinal mode is, however, increased with the controller on. This is partially explained by close examination of the optimized closed loop response in Figure 13, which also shows increased pitch rate over the open loop. Many factors associated with the testing and with the hardware implementation may also explain the increase. Further testing is required to provide a more comprehensive comparison.

### Summary

This paper describes a flight vehicle developed with a distributed control architecture based upon Miniature Trailing Edge Effectors (MiTEs). The details of

the demonstrator, including the vehicle configuration, distributed architecture, and hardware are provided. The controller synthesis approach based upon Probability Collectives theory was discussed. Details were provided of the theory and its application to the design of nonlinear, robust, distributed controllers. The results of distributed controller designs were presented. Flight tests were performed to characterize the response of the demonstrator and the distributed flight control architecture. Results of initial closed loop tests with a distributed stability augmentation system were also provided.

## Acknowledgements

This work was partially funded by NASA Langley Research Center.

## References

- <sup>1</sup>Nae, C., "Synthetic Jet Influence on NACA 0012 Airfoil at High Angles of Attack," AIAA Paper 98-4523.
- <sup>2</sup>Seifert, A., Darabi, A., Wagnanski, I., "Delay of Airfoil Stall by Periodic Excitation," Journal of Aircraft, Vol. 32, No. 4, July-August 1996.
- <sup>3</sup>Kroo, I., Eaton, J., Prinz, F., "UAV Aeroelastic Control Using Redundant Microflaps," Air Force Office of Scientific Research Program Review for Year I, 1999.
- <sup>4</sup>Kroo, I., "Aerodynamic Concepts for Future Aircraft," 30th AIAA Fluid Dynamics Conference (AIAA 99-3524), Norfolk, Va, June-July 1999.
- <sup>5</sup>Solovitz, S., Eaton, J.K., "Aeroelastic Control Using Redundant Microactuators," 3rd ASME/JSME Joint Fluids Engineering Conference, July 18-23, 1999, San Francisco, CA.
- <sup>6</sup>Liebeck, R. H., "Design of Subsonic Airfoils for High Lift," Journal of Aircraft, Vol. 15, No. 9, Sept., 1978.
- <sup>7</sup>Jeffrey, D., Zhang, X., and Hurst, D.W., "Aerodynamics of Gurney Flaps on a Single-Element High-Lift Wing," Journal of Aircraft, Vol. 37, No. 2, 2000, pp. 295-301.
- <sup>8</sup>Storms, B. L, and Jang, C. S., "Lift Enhancement of an Airfoil Using a Gurney Flap and Vortex Generators," Journal of Aircraft, Vol. 31, No. 3, June 1994.
- <sup>9</sup>Jang, C.S., Ross, J. C., and Cummings, R. M., "Computational Evaluation of an Airfoil with a Gurney Flap", AIAA Paper 92-2708, June 1992.
- <sup>10</sup>Lee, H. and Kroo, I., "Computational Investigation of Airfoils with Miniature Trailing Edge Control Surfaces" AIAA 2004-1051, Presented at 42nd AIAA Aerospace Sciences Meeting and Exhibit, Reno, Nevada, January 2004.
- <sup>11</sup>Bieniawski, S. and Kroo, I., "Flutter Suppression Using Micro-Trailing Edge Effectors," AIAA 2003-1941, 44th AIAA/ASME/ASCE/AHS Structures, Structural Dynamics, and Materials Conference, Norfolk, Virginia, 7-10 April 2003.
- <sup>12</sup>M. Kinzel, M. Maughmer and G. Lesieutre, "Numerical Investigation of Miniature Trailing-Edge Effectors on Static and Oscillating Airfoils," AIAA-2005-1039 Presented at 43rd AIAA Aerospace Sciences Meeting and Exhibit, Reno, Nevada, Jan. 10-13, 2005.
- <sup>13</sup>D. T. Yen Nakafuji, C. P. van Dam, J. Michel, and P. Morrison, "Load control for turbine blades - A non-traditional microtab approach," AIAA-2002-54 Presented at 2002 ASME Wind Energy Symposium; 40th AIAA Aerospace Sciences Meeting and Exhibit, Reno, NV, Jan. 14-17, 2002.
- <sup>14</sup>Tumer, K., Agogino A., and Wolpert, D. H., "Learning sequences of actions in collectives of autonomous agents," In *Proceedings of the First International Joint Conference on Autonomous and Multi-Agent Systems*, Bologna, Italy, July 2002.
- <sup>15</sup>Wolpert, D. H., Tumer, K., "Collective Intelligence, Data Routing, and Braess' Paradox," Journal of Artificial Intelligence Research, 2002.
- <sup>16</sup>Wolpert, D.H., Wheeler, K., Tumer, K., "Collective Intelligence for Control of Distributed Dynamical Systems," Europhysics Letters, vol. 49 issue 6, 708-714, 2000.
- <sup>17</sup>Wolpert, D.H., "Information theory - the bridge connecting bounded rational game theory and statistical physics", in *Complex Engineering Systems*, D. Braha, Ali Minai, and Y. Bar-Yam (Editors), Perseus books, in press.
- <sup>18</sup>Wolpert, D.H., Bieniawski, S., "Distributed Control by Lagrangian Steepest Descent" 43rd IEEE Conference on Decision and Control, December 2004.
- <sup>19</sup>Bieniawski, S., Wolpert, D.H., "Adaptive, distributed control of constrained multi-agent systems," in *Proceedings of the Third International Joint Conference on Autonomous Agents and Multiagent Systems (AAMAS 2004)*, 19-23 July 2004, New York, New York.
- <sup>20</sup>Macready, W., and Wolpert, D., "Distributed Optimization," International Conference on Complex Systems, Boston, May 2004.
- <sup>21</sup>Bieniawski, S., Wolpert, D.H., Kroo, I., "Discrete, Continuous, and Constrained Optimization Using Collectives," AIAA 2004-4580, 10th AIAA/ISSMO Multidisciplinary Analysis and Optimization Conference, Albany, New York, 30 August - 1 September 2004.
- <sup>22</sup>Henke, R., "Validation of Wing Technologies on an Airbus A 340 Flying Testbed: First Flight Test Results from the European Program AWIATOR", 24th Congress of the International Council of the Aeronautical Sciences, Yokohama, Japan, 29 August - 3 September 2004.
- <sup>23</sup>Lin Air, Desktop Aeronautics, P.O. Box 9937, Stanford, CA, 94305.
- <sup>24</sup>Ashley, H., **Engineering Analysis of Flight Vehicles**, Dover Publications, New York, 1974.
- <sup>25</sup>Tigner, B., Meyer, M., Holden, M., Page, M., Watson, W., Kroo, I., "Test Techniques for Small-Scale Research Aircraft," In 16th Applied Aerodynamics Conference, AIAA Paper 98-2726, June 1998.
- <sup>26</sup>Sutton, R.S., and Barto, A.G., **Reinforcement Learning**, MIT Press, Cambridge, MA, 2002.
- <sup>27</sup>Bieniawski, Stefan, "Distributed Optimization and Flight Control Using Collectives," Doctoral Thesis, Stanford University, 2005.